RESEARCH ARTICLE

Key Points:
- Identical polarity of penetration electric field over Thumba and Jicamarca
- Role of IMF B_y in determining polarity of prompt penetration electric field
- Changes in IMF B_y distort DP2 cells to bring antipodal stations (Thumba and Jicamarca) in the same cell

Correspondence to:
D. Chakrabarty,
dipu@prl.res.in

Role of IMF B_y in the prompt electric field disturbances over equatorial ionosphere during a space weather event

D. Chakrabarty[1] [ID]**, Debrup Hui[1]** [ID]**, Diptiranjan Rout[1]** [ID]**, R. Sekar[1]** [ID]**, Archana Bhattacharyya[2]** [ID]**,
G. D. Reeves[3,4] [ID]**, and J. M. Ruohoniemi[5]** [ID]

[1]Physical Research Laboratory, Ahmedabad, India, [2]Indian Institute of Geomagnetism, Navi Mumbai, India, [3]Los Alamos National Laboratory, Los Alamos, New Mexico, USA, [4]New Mexico Consortium, Los Alamos, New Mexico, USA, [5]Bradley Department of Electrical and Computer Engineering, Virginia Polytechnic Institute and State University, Blacksburg, Virginia, USA

Abstract On 7 January 2005 ($A_p = 40$) prompt penetration electric field perturbations of opposite polarities were observed over Thumba and Jicamarca on a few occasions during 13:45–16:30 UT. However, the electric field was found to be eastward during 14:45–15:30 UT over both Thumba and Jicamarca contrary to the general expectation wherein opposite polarities are expected at nearly antipodal points. On closer scrutiny, three important observational features are noticed during 14:10–15:15 UT. First, during 14:10–14:45 UT, despite increasing southward interplanetary magnetic field (IMF) B_z condition, the already westward electric field over Thumba weakened (less westward) while the eastward electric field over Jicamarca intensified (more eastward). Second, the electric field not only became anomalously eastward over Thumba but also got intensified further during 14:45–15:00 UT similar to Jicamarca. Third, during 15:00–15:15 UT, despite IMF B_z remaining steadily southward, the eastward electric field continued to intensify over Thumba but weakened over Jicamarca. It is suggested that the changes in IMF B_y component under southward IMF B_z condition are responsible for skewing the ionospheric equipotential patterns over the dip equator in such a way that Thumba came into the same DP2 cell as that of Jicamarca leading to anomalous electric field variations. Magnetic field measurements along the Indian and Jicamarca longitude sectors and changes in high-latitude ionospheric convection patterns provide credence to this proposition. Thus, the present investigation shows that the variations in IMF B_y are fundamentally important to understand the prompt penetration effects over low latitudes.

1. Introduction

The space weather event (7 January 2005) which is addressed in the present work was first presented [*Chakrabarty et al.*, 2006] in the context of providing an evidence for triggering of an equatorial spread *F* (ESF) event and premidnight resurrection of a plasma plume under the influence of the effects of *Y* component of interplanetary electric field (IEFy) over the Indian sector. The onset of equatorial spread *F* in the postsunset period and premidnight resurrection of plasma plume on this night were believed to be due to eastward electric field perturbations associated with the prompt penetration and overshielding effects of IEFy respectively. The role of eastward overshielding electric field in the premidnight resurrection of the plasma plume on this night was also discussed in *Sekar and Chakrabarty* [2008] based on 2-D nonlinear numerical simulation investigations. In the work of *Chakrabarty et al.* [2006], the eastward electric field perturbations due to the prompt penetration and overshielding effects separated by about an hour were shown to be associated with the southward and northward excursions of interplanetary magnetic field (IMF) B_z. Thus, the earlier investigations were focused on the effects of prompt penetration and overshielding electric fields on the equatorial ionosphere over the Indian sector. However, it remained a conundrum (and not addressed earlier) as to how the polarity of prompt penetration and overshielding electric fields could be same (i.e., eastward) on this occasion if the over-shielding electric field is considered as a counteracting field that became dominant (in the inner magnetosphere) once the prompt penetration field was withdrawn. An attempt is made in this work to resolve this conundrum by comparing the drift variations with the quiet time variations. More importantly, the drift data from Jicamarca on the same day are also presented in this work to bring out the possible roles of IMF B_y. In order to rule out the influences of other factors, the variations in the solar wind dynamic pressure and substorm activity are also investigated.

The role of IMF B_z in the prompt penetration of interplanetary electric field into equatorial ionosphere is well known and there have been many investigations [*Vasyliunas*, 1970; *Wolf and Jaggi*, 1973; *Kikuchi et al.*, 2008, 2010; *Chakrabarty et al.*, 2015] that addressed this aspect. It is generally expected that the polarity of the prompt penetration electric field perturbation is eastward till ∼22:00 LT and westward in the postmidnight hours [e.g., *Nopper and Carovillano*, 1978]. The polarity of the overshielding electric field perturbation is expected to be opposite, i.e., westward during daytime [*Simi et al.*, 2012] and eastward [*Chakrabarty et al.*, 2006] during nighttime over equatorial ionosphere. Therefore, opposite polarities of prompt penetration electric field are expected [e.g., *Gonzales et al.*, 1979] during day and nighttime at a given place over the dip equatorial region. For nearly antipodal locations like Jicamarca and Thumba that are dip equatorial stations over the Peruvian and Indian sectors, respectively, *Kelley et al.* [2007] showed that the polarities of the prompt penetration electric field perturbations are opposite. This is, in general, consistent with the curl-free condition of the ionospheric electric field. Therefore, *Kelley et al.* [2007] rightly pointed out that in a geomagnetic coordinate system, the zonal components of the prompt penetration electric field has the opposite polarities in the dayside vis-à-vis the nightside. However, it remained to be investigated how changes in IMF B_y during steady southward IMF B_z condition modifies this arrangement with regard to the response of the equatorial ionosphere particularly around postsunset and morning hours. The present investigation provides such an example.

2. Results

Figure 1 shows the variations in the solar wind and geomagnetic parameters as well as the effects on equatorial ionosphere over the Indian (Thumba, TVM: 8.5°N; 77°E and dip: 0.5° N) and Peruvian (Jicamarca, JIC: 11.9°S; 76.8°W and dip: 0.8°N) sectors during the space weather event (7 January 2005) under consideration. Figure 2 helps to rule out any substorm-related prompt electric field perturbations during the interval under consideration. Other figures are presented in the discussion section to support the proposition suggested in this communication.

Figure 1 consists of six (a–f) subplots with five shaded regions to mark the intervals when the prompt penetration (PP) processes are characteristically different. The solar wind data are taken from NASA Goddard Space Flight Center (GSFC) Coordinated Data Analysis Web (CDAWeb) (http://cdaweb.gsfc.nasa.gov/) where these parameters are time shifted to the nose of the terrestrial bow shock. As this time shift matches well with the observed high-latitude ionospheric plasma convection patterns (ionospheric footprints), additional shift is not provided for this event to account for other processes like the magnetosheath and Alfvén transit times *Chakrabarty et al.* [2005]. *Bhaskar and Vichare* [2013] have shown that these transit times can be occasionally negligible. The *SYM-H* data (in cyan) are taken from World Data Center-C2 (Kyoto). Plasma drift data from JULIA (Jicamarca Unattended Long-term Investigations of the Ionosphere and Atmosphere) radar at Jicamarca, Peru, are used in the present investigation. JULIA radar measures plasma drifts from the Doppler shifts of coherent echoes received from the daytime 150 km region irregularities. The vertical drift measured with this technique is shown to be the proxy for the ambient zonal electric field over the dip equatorial region [*Kudeki and Fawcett*, 1993]. The collection and description of plasma drift data using JULIA are detailed in *Fejer* [2011] and *Hui and Fejer* [2015]. Further, temporal variations in h'F (base height of the ionospheric F layer) over Thumba, India, are used to derive the F region vertical plasma drifts after correcting for the chemical recombination as suggested by *Bittencourt and Abdu* [1981]. The derivation of vertical plasma drifts from the measurements of h'F over Thumba is described in detail in *Chakrabarty et al.* [2006]. In this work, Figure 1f is reproduced from *Chakrabarty et al.* [2006] with X axis represented in LT (LT = UT + 5:08 h) instead of Indian Standard Time (IST = UT + 5:30 h). The uncertainties associated with the JULIA and Thumba plasma drifts are < 2 and ∼5 m/s, respectively. For the plasma drifts data, positive values represent upward drifts corresponding to eastward electric field. All the parameters in Figure 1 have 1 min temporal resolution except the JULIA and the Thumba vertical plasma drifts for which the cadences are 5 min and 15 min, respectively. The plasma drifts discussed in Figures 1e and 1f correspond to the resultant plasma drift which is algebraic sum of drifts due to quiet time dynamo and perturbation drifts of external origin. While the top X axis in Figure 1a denotes the time in UT, the corresponding LTs for Figures 1e and Figure 1f are marked at the corresponding bottom X axes. Five time tags (T_1, T_2, T_3, T_4, and T_5) are used for convenience in Figure 1 that are shown along the X axis of Figure 1c. In terms of UT, the five time tags stand for 13:37, 14:10, 15:00, 15:15, and 15:54 h. These time tags represent
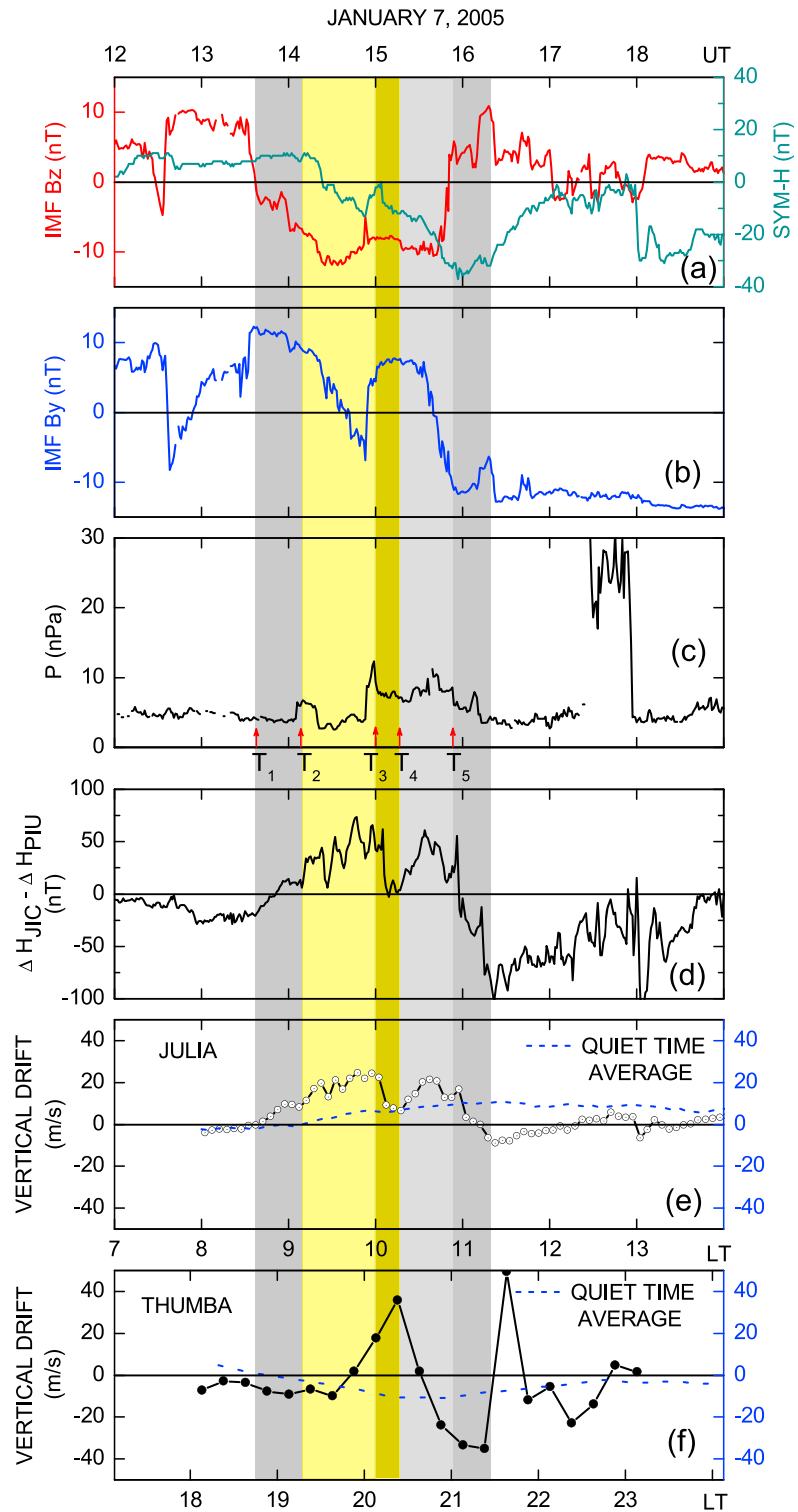
Figure 1. The variations in (a) IMF B_z (in red) and *SYM-H* (in cyan), (b) IMF B_y (in blue), (c) solar wind pressure *P*, on 7 January 2005. These variations are compared with the (d) EEJ variations over Peruvian sector ΔH_{JIC}-ΔH_{PIU}, (e) vertical plasma drift from JULIA (in black) along with its four quiet day average prior to the event (in dashed blue), and (f) vertical drift data over Thumba (in black) after *Chakrabarty et al.* [2006] along with its seasonal quiet time values from *Madhav Haridas et al.* [2015] (in dashed blue). The Jicamarca and Thumba drifts have uncertainties of the order of 2 m/s and 5 m/s, respectively. The vertical plasma drifts are proxy for ionospheric zonal electric fields. Upward (downward) drifts represent eastward (westward) electric field. T_1 through T_5 are time tags that separate the different shaded regions on the plot and are used for convenience to identify different dominant processes governing the plasma drifts.
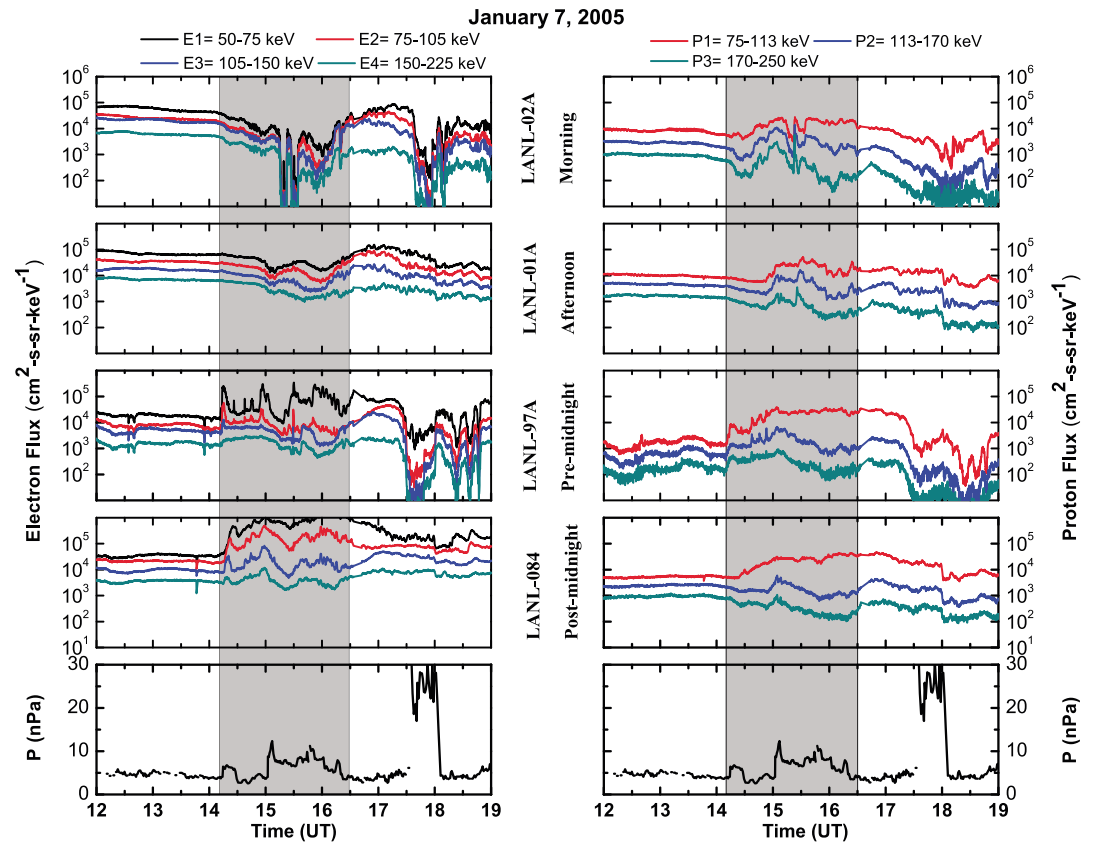
Figure 2. The variations in LANL-02A (morning), LANL-01A (afternoon), LANL-97A (premidnight), and LANL-084 (postmidnight) geosynchronous (left column) electron and (right column) proton fluxes for different energy channels. The variations in solar wind pressure P is also shown at the bottom of both the panels for convenience. The shaded region highlights the interval wherein changes in P are observed during the period of interest.

08:37, 09:10, 10:00, 10:15, and 10:54 LT over Jicamarca and 18:45, 19:18, 20:08, 20:23, and 21:02 LT over Thumba. In this work, a notation of $T_{i(i=1,2,\ldots,5)} \pm$ hh:mm is used to indicate hour(hh):minutes(mm) past/prior to the time tag "T_i."

Figure 1a shows that IMF B_z changed polarity and turned southward (negative) at T_1. It gradually intensified (barring occasional ephemeral weakening) during the interval between T_1 and (T_2 + 00:15) and became less southward between (T_2 + 00:15) and T_3. During the interval $T_1 - T_2$, although IMF B_y magnitude is large and positive, southward IMF B_z magnitude is relatively smaller. The variations in SYM-H in Figure 1a shows development of the main phase of a minor geomagnetic storm in response to the southward IMF B_z condition. At (T_2 + 00:30), when IMF B_z was southward, IMF B_y changed polarity (Figure 1b) from dusk to dawnward direction (changed sign from "+" to "−"). This was relatively a gradual change compared to the second one during (T_3 − 00:10) – T_3, which was an abrupt change from the dawn to duskward direction (changed sign from − to +). Figure 1c reveals two enhancements in solar wind ram pressure during the interval (T_2 − 00:05) to T_3. The amplitude of the pressure pulse at (T_2 − 00:05) was smaller than that which started around (T_3 − 00:10). The pressure pulse at (T_3 − 00:10) took the ram pressure to an elevated level till (T_5 + 00:30). Figure 1d shows the variations in $\Delta H_{JIC} - \Delta H_{PIU}$ which is a proxy for the strength of equatorial electrojet (EEJ) based on the magnetometer observations from a dip equatorial (Jicamarca) and an off-equatorial (Piura, PIU: 5.17°S, 80.64°W and dip: 6.8°N) station over the Peruvian sector. It can be noted that $\Delta H_{JIC} - \Delta H_{PIU}$ became positive during $T_1 - T_2$ and increased during $T_2 - T_3$ to cross +50 nT.

Figure 1e reveals that JULIA drifts were significantly upward in both the intervals $T_1 - T_2$ and $T_2 - T_3$ that caused substantial departure of the variations in drifts from the average quiet day drift pattern (blue dashed line) constructed from four quiet days (23, 24, 26, and 27 December 2004) drifts prior to the event day. The positive deviation of the JULIA drifts during the interval $T_1 - T_2$ indicates an eastward PP electric field perturbation.

This deviation becomes even more pronounced during $T_2 - T_3$ when the JULIA drifts became significantly upward (more than 20 m/s). This clearly points toward the influence of an eastward PP electric field perturbation during the interval $T_2 - T_3$. Over Thumba, on the other hand, the F region vertical drifts were downward during the interval $T_1 - T_2$, less downward (approaching zero) during $T_2 - (T_2 + 00:35)$, and significantly upward ($\sim$20 m/s) during the time interval $(T_2 + 00:35) - T_3$. The drifts during $(T_2 + 00:20) - T_3$ were in sharp contrast to the average vertical drifts (blue dashed line) at this local time reported by *Madhav Haridas et al.* [2015] based on h'F observations. The deviation of the Thumba drift was above the uncertainty level ($\sim$5 m/s) during the interval $T_1 - T_2$, and it was consistently negative in contrast to the quiet time drifts suggesting a westward PP electric field influence during $T_1 - T_2$. However, after $(T_2 + 00:20)$, Thumba started experiencing an eastward electric field perturbation although this was not able to change the westward polarity till $(T_2 + 00:35)$. It can also be noted that the deviations of the Thumba drifts during $T_1 - (T_2 + 00:20)$ with respect to the average variation are almost of the same magnitude as those of the Jicamarca drifts with respect to the average variation although the sense is opposite. It is difficult to delineate the contribution of the small pressure pulse at $(T_2 - 00:05)$ in the electric field perturbation over the equatorial ionosphere as it occurred concurrently with the southward IMF B_z condition when eastward/westward electric field perturbations were observed over Jicamarca/Thumba. During the interval $(T_2 + 00:35) - T_3$, the vertical drifts over both Thumba and Jicamarca were positive (upward) indicating an eastward electric field perturbation over both the stations throughout the interval $(T_2 + 00:35) - T_3$. This was concomitant with southward IMF B_z condition and the very sharp polarity reversal in IMF B_y in between $(T_3 - 00:10) - T_3$ from dawn to duskward direction. Interestingly, the rate of enhancement of the drifts was also positive during this time over both the sectors. The identical polarity of prompt penetration electric field in both morning and post sunset sectors in the interval $(T_2 + 00:35) - T_3$ is very unusual and in sharp contrast to the expected opposite polarity [e.g., *Gonzales et al.*, 1979; *Kelley et al.*, 2007] over these two sectors. This IMF B_y event was also accompanied by the arrival of a solar wind pressure pulse. This pressure pulse started at the same time as that of the sharp and positive IMF B_y excursion. However, it took the ram pressure to an elevated level only after T_3 that continued till $(T_5 + 00:30)$. This pressure pulse does not seem to have affected the polarity of the daytime electric field over Jicamarca significantly as westward electric field perturbations were observed during this time over Jicamarca in contrast to the eastward electric field perturbations expected based on the results reported by *Huang* [2008]. It can additionally be noted that at $(T_2 + 00:30)$, IMF B_y changed polarity from dusk (positive) to dawnward (negative) direction and remained dawnward for about 10 min. During this time, IMF B_z became slightly less southward. However, the net upward rise in Thumba drift does not seem to get affected by the negative IMF B_y perhaps due to 15 min temporal resolution of Thumba drift data.

During $T_3 - T_4$, IMF B_z remained steadily southward and IMF B_y slowly became more duskward (more positive). Figure 1d reveals that $\Delta H_{JIC} - \Delta H_{PIU}$ decreased sharply and touched almost zero level during $T_3 - T_4$, while Figure 1e shows that JULIA drift also decreased sharply by more than 15 m/s during this time. Although the polarity of the electric field (corresponding to the observed drifts) was still eastward over Thumba and Jicamarca, the decrease in the magnitude of the upward drift suggests westward electric field perturbation in the interval $(T_3 - T_4)$ over Jicamarca. In contrast, and very importantly, the upward drift over Thumba shows further enhancement (by $\sim$15 m/s) suggesting influence of an eastward electric field perturbation. Therefore, electric field perturbations of opposite polarities were observed over Thumba and Jicamarca sectors between T_3 and T_4.

After T_4, IMF B_y remained steady for about 15 min and IMF B_z also remained steadily southward for about 25 min. No ram pressure spike is seen during this time. At this time, eastward electric field perturbations were felt over Jicamarca as $\Delta H_{JIC} - \Delta H_{PIU}$ again increased to +50 nT level and JULIA drifts increased to $\sim$+20 m/s. The JULIA drifts at this time were almost twice the average quiet day values ($\sim$+10 m/s) suggesting an eastward electric field perturbation. Interestingly, the drift at Thumba started decreasing from T_4 and after 15 min, the drifts became downward. At around 16:00 UT, the drifts are found to be significantly downward ($\sim$−35 m/s). This suggests a westward electric field perturbation over Thumba. Therefore, these observations reveal eastward penetration electric field over Jicamarca and westward penetration electric field over Thumba for about half an hour after T_4. This is similar to what happened during $T_1 - T_2$ with the exception that the westward electric field magnitude was now much larger over Thumba. It is also interesting to note that southward IMF B_z was much stronger (nearly double) during $T_4 - (T_4 + 00:25)$ compared to that during $T_1 - T_2$. IMF B_y changed polarity at $(T_4 + 00:20)$ and crossed −10 nT at T_5 which is larger compared to the similar excursion

at (T_2 + 00:30). However, IMF B_z started flipping direction (southward to northward) abruptly from (T_4 + 00:25) onward and eventually became northward just before T_5 giving rise to an overshielding condition.

In response to the overshielding condition, $\Delta H_{JIC} - \Delta H_{PIU}$ sharply decreased at T_5 and also 20 minutes after T_5 that took the minimum value of $\Delta H_{JIC} - \Delta H_{PIU}$ to reach $\sim$−100 nT at (T_5 + 00:30). This suggests a strong counter electrojet (CEJ) condition over the American sector. JULIA drifts also decreased at T_5, changed polarity at (T_5 + 00:20), and became significantly downward ($\sim$−10 m/s) at (T_5 + 00:30). It can be noted that the JULIA drift at (T_5 + 00:30) was significantly different from the average quiet day pattern. On the other hand, the downward F region drifts at Thumba started slowing down after T_5 indicating influence of eastward overshielding electric field and changed polarity at around (T_5 + 00:30). Although the change of polarity over Thumba seems to be a little delayed ($\sim$10 min), this may be due to the coarse temporal resolution of the Thumba drift data. Nevertheless, the drift over Thumba became significantly upward ($\sim$40 m/s) at around (T_5 + 00:40). It can also be noted that the significantly upward drift over Thumba at this local time was in sharp contrast with the average quiet day pattern. Expectedly, the polarities of the overshielding electric field perturbations over Thumba and Jicamarca were opposite. It is of interest to note here that the complete overshielding process took place in two steps separated by $\sim$20 min wherein IMF B_z initially turned northward (from stable southward condition) at T_5 and further northward at (T_5 + 00:20). The equatorial vertical drift perturbations over both Thumba and Jicamarca seem to have responded simultaneously to this two-step overshielding process.

As mentioned earlier, it is important to rule out substorm-induced electric field perturbations [e.g., *Chakrabarty et al.*, 2010, 2015] during this event to assess the role of IMF B_y. It is generally accepted that "dispersionless" particle injection at the geosynchronous orbit is a telltale signature [e.g., *Reeves et al.*, 2003] of substorm onset whereas enhancements in the solar wind ram pressure cause undulations in the geosynchronous particle flux which is different from substorm signatures [*Lee et al.*, 2005]. Therefore, Figure 2 is plotted to show the variations in the geosynchronous energetic particle (both electron and proton) fluxes along with solar wind ram pressure during 12:00–19:00 UT. Figure 2 represents the variations in the electron and proton fluxes for different energy channels as observed by the LANL (Los Alamos National Laboratory) satellites LANL-02A, LANL-01A, LANL-97A, and LANL-084 that were on the morning, afternoon, premidnight, and postmidnight sectors, respectively. To facilitate comparison, Figure 2 (fifth row), representing variations in the solar wind ram pressure, is reproduced from Figure 1c. It is of interest to note that variations in the geosynchronous particle fluxes were in sync with elevated ram pressures during the shaded interval. In addition, the dispersionless particle injection was absent in the nightside. These clearly suggest that the geosynchronous particle flux signatures were not due to substorms and are caused by changes in the solar wind ram pressure [*Lee et al.*, 2005]. Thus, the variations observed in the plasma drifts over Jicamarca and Thumba were not associated with substorm. Therefore, this aspect will not be discussed further.

3. Discussion

A careful consideration of the PP electric field perturbations during $T_4 - T_5$ and overshielding electric field during $T_5 - (T_5 + 00:30)$ suggests that the polarity of the second one was opposite compared to the polarity of the PP electric field over both Indian and Peruvian sectors. Therefore, the overshielding electric field effect described here is not in response to the PP electric field corresponding to those during $T_2 - T_3$, as was originally believed [e.g., *Chakrabarty et al.*, 2006]. Rather, the overshielding electric field (eastward over Thumba) during $T_5 - (T_5 + 00:40)$ originated to counter the PP electric field (westward over Thumba) during $T_4 - T_5$. This solves the conundrum described in section 1.

During the course of events between T_1 and (T_5 + 00:30), opposite PP electric field perturbations are experienced over Thumba and Jicamarca during ($T_1 - T_2$), ($T_4 - T_5$), and during $T_5 - (T_5 + 00:30)$ when the overshielding took place. The opposite PP electric field perturbation over Thumba and Jicamarca during ($T_1 - T_2$) and ($T_4 - T_5$) are consistent with *Kelley et al.* [2007]. However, westward polarity of the PP electric field over Thumba during postsunset hours is counterintuitive based on earlier results. The local time dependence of longitudinally averaged equatorial PP vertical plasma drifts in *Fejer et al.* [2008a] shows eastward prompt penetration electric field till 22:00 LT during winter solstice over the dip equatorial latitudes. The work of *Fejer et al.* [2008a] is also in agreement with the modeling results [e.g., *Nopper and Carovillano*, 1978; *Senior and Blanc*, 1984; *Tsunomura and Araki*, 1984; *Maruyama et al.*, 2005]. Therefore, the westward polarity of the PP electric field over the Indian sector before 22:00 LT in the present case is in contrast with the earlier results. However, the

ensuing discussion will indicate that the interplay of southward IMF B_z and state of IMF B_y may decide the polarity of PP electric field over equatorial ionosphere.

Before looking at the drifts during $T_2 - T_4$, it is worthwhile to look into the observations of the northward (X) component of the geomagnetic field obtained from SuperMAG network (http://supermag.jhuapl.edu) to understand coupling between high and low latitudes. The ΔX variations for a given station is obtained after subtracting the nighttime base level. A comparison of the variations in ΔX during 13:30 – 16:00 UT at the corresponding (nearly same latitudes) stations along the Indian and Jicamarca longitude regions is made in Figures 3a – 3d. The magnetic latitude and longitude (in AACGM coordinates using IGRF-2010 model) of each station are also mentioned in Figure 3. The stations lying along the Indian longitude are Novosibirsk (NVS), Irkutsk (IRT), Lanzhou (LZH), Alibag (ABG), and Tirunelveli (TIR) whereas the stations along the Jicamarca longitude are Ottawa (OTT), Fredericksburg (FRD), Teoloyucan (TEO), and Huancayo (HUA). It is also to be noted that because of unavailability of data from any nearby station, the longitude of the station TEO is slightly different from the longitudes of other stations (OTT, FRD, and HUA) along the Jicamarca sector. The variations in IMF B_z and B_y are reproduced in Figure 3 from Figure 1 to facilitate comparison. In order to draw attention to a very interesting feature during the period $T_2 - T_4$, a rectangular shaded (in cyan) box is superimposed on the subplots. In this particular interval, the pair of magnetic midlatitude stations (OTT-NVS as well as FRD-IRT) show predominantly out-of-phase variations but as one come closer to low (TEO-LZH, note TEO is also slightly offset in magnetic longitude) and equatorial (HUA-ABG-TIR) latitudes, the ΔX variations reveal increasingly in-phase variations. This feature is absent before T_2 and after T_4. This strongly indicates that the equatorial stations were within the same DP2 cell (to be discussed later) during this period and not on other occasions. It is also apparent that the magnetic midlatitude stations were on two different cells. It is important to mention in this context that Indian longitude sector was on nightside during this period when ionospheric conductivity is low to support significant current. Therefore, ionospheric contribution in ΔX variations over the Indian longitude region can be debated. However, considering the fact that IMF B_z, B_y, and other solar wind parameters do not show similar fluctuations as those seen in ΔX during 14:25 – 15:10 UT over Indian equatorial region, the ionospheric origin of these variations can be inferred. Further, based on concomitant variations in ionospheric plasma drift and ground-based nocturnal horizontal magnetic field measurements, *Rastogi et al.* [1996] inferred that a finite current flows in the nocturnal dip equatorial ionosphere which gets further credence from the recent works of *Pandey et al.* [2016]. Therefore, the similarity in ΔX variations between TIR and HUA strongly points toward the locations of these stations within the same DP2 ionospheric cell during $T_2 - T_4$.

As indicated earlier and supported by the magnetic observations, the PP electric field perturbations during $T_2 - T_4$ deserve special attention. This is because equatorial ionosphere over Thumba experienced eastward PP electric field perturbation during the $(T_2+00:20) - T_4$, while intervals just before and after this, it experienced westward PP electric field perturbation. In addition, the polarity of resultant plasma drifts during $(T_2+00:35) - (T_4+00:15)$ over Thumba is opposite to the nighttime (downward) polarity expected during magnetically quiet periods. It is important to note that during $T_1 - T_2$, while IMF B_y was positive and of considerable magnitude (∼10 nT), IMF B_z was still turning toward south with its magnitude less than IMF B_y during this interval. Therefore, it is expected that strength of the DP2 convection electric field, primarily driven by IMF B_z, over Thumba (in this case, westward) was small. As southward IMF B_z increased in strength during $T_2 - (T_2+00:20)$, the drifts over Thumba remained downward. It is also possible that during $T_1 - (T_2+00:20)$ westward PP due to increasing IMF B_z competed with the eastward effects due to IMF B_y resulting into reduced magnitude of westward PP. However, during $(T_2+00:20) - (T_2+00:35)$, when the southward IMF B_z remained relatively steady, the effects (eastward) of positive IMF B_y comes into play and as a consequence, the equatorial ionosphere over Thumba experienced a eastward PP influence. Clearly, as IMF B_y magnitude was less during this interval, it could not change the polarity of the electric field to eastward direction over Thumba. However, during $(T_2+00:35) - T_3$, as the magnitude of southward IMF B_z decreases and IMF B_y sharply changes its polarity from dawnward (−) to duskward (+) direction, Thumba experienced a clear eastward electric field influence. Opposite changes in electric field, if any, owing to the negative IMF B_y polarity from about $(T_2+00:30)$ for about 10 min is either canceled by the reduction in the strength of southward IMF B_z or not captured by Thumba drift data which has a temporal resolution of 15 min. In all likelihood, Thumba drift data captured the net upward changes (or net eastward electric field changes) during this time with data cadence of 15 min. During $T_3 - T_4$, as IMF B_z remained steadily southward and IMF B_y increased to more positive values, Thumba experienced intensification of the eastward electric field perturbation. Interestingly, Jicamarca which showed enhanced upward drifts as expected on the day sector all along $T_1 - T_3$ started showing westward PP electric field influence in
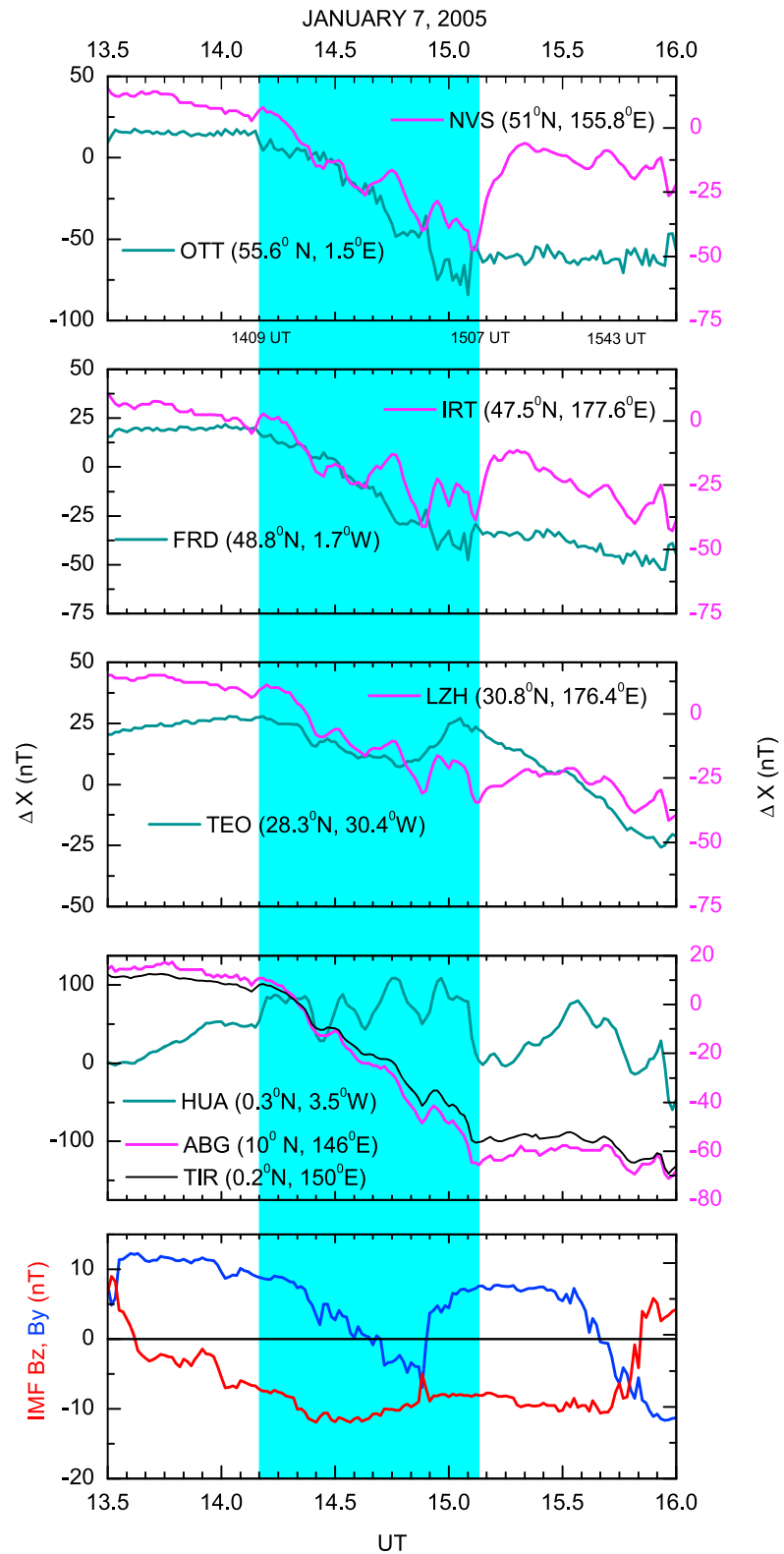
Figure 3. The ΔX component of magnetic field from high to low latitudes along the Jicamarca and Indian longitude sectors is shown. The stations along the Jicamarca sector are labeled on the left (in cyan) and the stations along the Indian sector are shown on the right (in magenta). In the bottom panel are shown IMF B_z (in red), and By (in blue). The shaded region marks the period when IMF B_y is changing. In the shaded region, the magnetic data from Jicamarca and Indian sectors show anti-correlation at high latitudes but become correlated at low latitudes.

the interval $T_3 - T_4$. Significant westward PP influence during $T_4 - T_5$ over Thumba could be because of the westward PP due to the southward IMF B_z compounded by negative IMF B_y condition generating additional westward electric field influence.

The above discussion suggests possible role of IMF B_y especially over Thumba where eastward electric field got unusually strengthened during $T_2 - T_4$. *Tsurutani et al.* [2008] suggested that the polarity of the PP electric field perturbations over equatorial ionosphere can be complicated at local times other than the noon and midnight hours owing to the possible skewing and asymmetry between the DP2 convection vortices. IMF B_y can play an important role in the distortion of the DP2 convection patterns [*Heelis*, 1984; *Friis-Christensen et al.*, 1985; *Cumnock et al.*, 1992]. Over high latitudes, the change of sign of IMF B_y from dawn to duskward (dusk to dawnward) has been shown to affect the movement of the auroral arcs from dawn to dusk (dusk to dawn) direction [*Cumnock et al.*, 1997]. Further, bending polar arcs are also shown to be associated with the sign change in IMF B_y [*Kullen et al.*, 2015]. *Cumnock et al.* [1992] also showed that the high-latitude convection patterns under northward IMF B_z condition can change in a manner similar to what is expected if IMF B_z is southward when IMF B_y is large and changes slowly from dusk to dawnward direction (changes sign from + to −). Therefore, the changes in IMF B_y is expected to be effective in changing the convection patterns (DP2 cells) which reaches up to dip equatorial ionosphere under southward IMF B_z condition. In fact, the work of [*Heelis*, 1984] suggests that the convection patterns get highly distorted depending upon the magnitude and change in polarity of IMF B_y under southward IMF B_z condition. The above works suggest that the relative magnitudes of IMF B_z and IMF B_y determine the size of the DP2 convection cells and the polarity of IMF B_y decides the skewing effects. Therefore, it is suggested here that as far as the equatorial PP electric fields are concerned corresponding to southward IMF B_z, a favorable IMF B_y condition may bring the daytime prompt penetration electric field to dusk side and vice versa depending upon the skewing of the convection/equipotential patterns by IMF B_y. In other words, depending upon the IMF B_y condition, the dusk side may electrodynamically behave as dayside as the noon-midnight meridian no longer coincides with the electrodynamic divider of DP2 cells. *Nopper and Carovillano* [1978] points out that during disturbed times, the high-latitude field aligned currents can establish a strong "polar-equatorial coupling" which not only makes the low latitude fields fluctuate but also reverse their directions. It is believed that the unique situation during $T_2 - T_4$ wherein IMF B_y induced eastward electric field perturbation seen over Thumba during $T_2 - (T_2 + 00:35)$ that reduced the westward PP caused by increasingly southward IMF B_z, identical eastward polarity of PP electric field over Jicamarca and Thumba during $(T_2 + 00:35) - T_3$ and also enhancement (reduction) of eastward electric field perturbation over Thumba (Jicamarca) between $(T_3 - T_4)$ were greatly influenced by the changes in IMF B_y polarity under southward IMF B_z condition. The changes in the IMF B_y during these periods are believed to have rotated the DP2 cells in such a manner that Thumba started coming out of the dusk cell during $T_2 - (T_2 + 00:35)$, went into the dawn cell (same cell wherein Jicamarca is located) during $(T_2 + 00:35) - T_3$, and entered deeper into the dawn cell during $T_3 - T_4$, while Jicamarca tried to go out of it. This explains the electric field behavior over Thumba and Jicamarca during $T_2 - T_4$ subject to expected observations of DP2 cells at polar latitudes, which will be discussed later.

The dependence of DP2 cells on IMF clock angle has been studied both by simulation [e.g., *Heelis*, 1984; *Tanaka*, 2007] and with direct measurements over high latitudes [e.g., *Ruohoniemi and Greenwald*, 2005]. Under southward IMF B_z conditions, the dawn and dusk cells take what is usually referred to as circular (or orange) and crescent (or banana) shape and has distinctive antisunward throat and exit flows in between the cells. For strong IMF B_{y+}, the dusk cell expands into the dayside taking an orange shape and the dawn cell takes a crescent shape with the electrodynamic divider ($\Phi = 0$) rotating in clockwise direction from the unusual noon-midnight meridian characteristic of IMF $B_y \approx 0$. This results in an anticlockwise rotation of the throat flows and duskward zonal flows across the midnight sector. When IMF B_y changes to dawnward direction (-ve), the dawn cell starts taking the shape of an orange and the dusk cell changes to a banana with an overall anticlockwise rotation for both the cells. This results in the clockwise rotation of the throat flows and dawnward zonal flows on the midnight side. Figure 11 in *Tanaka* [2007] and Figure 7 in *Ruohoniemi and Greenwald* [2005] illustrate these features of the effects of changes in the IMF clock angles on the evolution of DP2 cells.

On the basis of above discussion and drawing inspiration from Figures 1 and 2 in *Nopper and Carovillano* [1978] and Figure 4 in *Heelis* [1984], a simplistic schematic is presented in Figure 4 corresponding to (a) IMF $B_y \approx 0$, (b) IMF B_{y+}, and (c) IMF B_{y-} conditions. The purpose of this schematic is to highlight a few possible characteristic features of the DP2 cells, equipotential patterns, and the location of the electrodynamic boundary
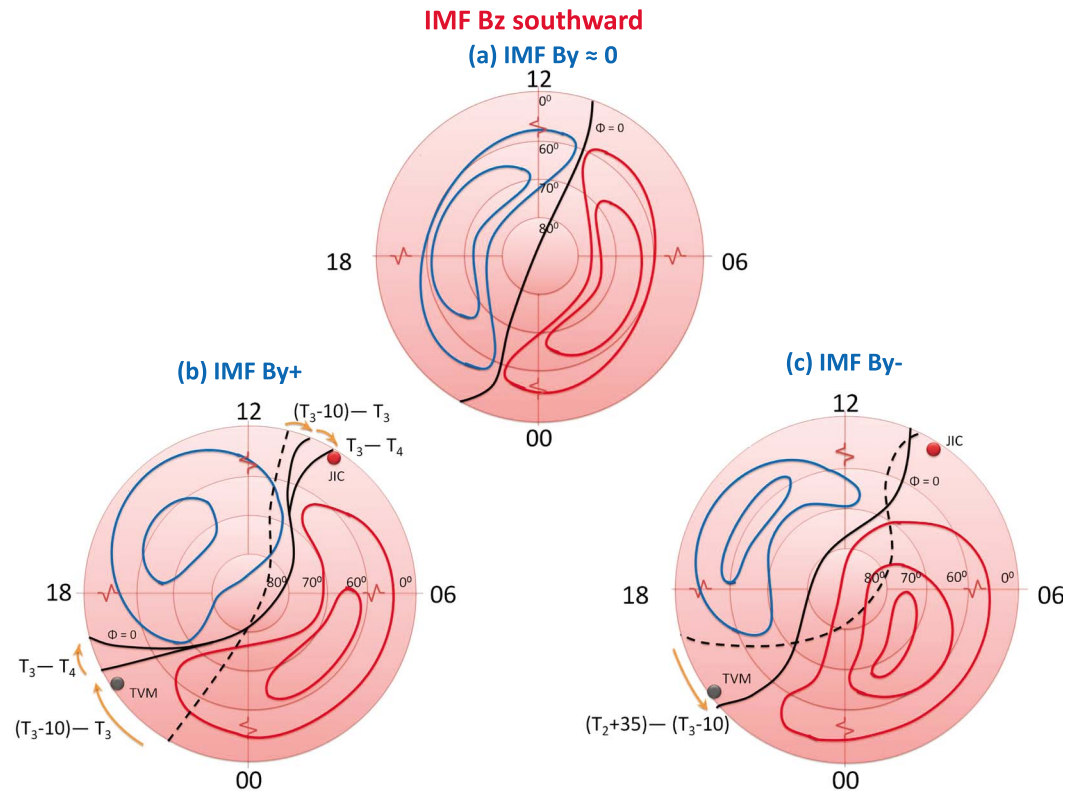
Figure 4. A schematic of the possible time evolution of the DP2 equipotential contours under southward IMF B_z condition with changes in IMF B_y polarity. The solid black lines represent the electrodynamical divider ($\Phi = 0$) between the dawn (red) and dusk (blue) cells which is tilted with respect to the noon-midnight meridian whereas the dotted black line represents the electrodynamical divider at previous condition. When (a) IMF $B_y \approx 0$, two symmetric cells, (b) when IMF B_y is duskward (positive), the electrodynamic divider undergoes a clockwise rotation and encompasses Thumba in the dawn cell, and (c) when IMF B_y is dawnward (negative), the electrodynamical divider undergoes an anticlockwise rotation. The curved arrows show how the electrodynamic divider is believed to have evolved with changing IMF B_y polarity in the mentioned time intervals. Please note that the change in Thumbs drifts for the scenario in Figure 4c during $(T_2 + 00:35)-(T_3 - 00:10)$ is probably not picked up by Thumba digisonde measurements (Figure 1f) owing to coarse temporal (15 min) resolution.

between the dawn and the dusk cells from polar and equatorial latitudes that can explain the electric field variations over Thumba and Jicamarca during $T_2 - T_4$. It is known that during disturbed times the high-latitude equipotential lines extend well up to the equatorial latitudes covering large local time sectors [*Nopper and Carovillano*, 1978; *Tsunomura*, 1999]. For southward IMF B_z, the DP2 dusk and dawn cells are symmetric but tilted [e.g., *Tanaka*, 2007] about the noon-midnight line when IMF $B_y \approx 0$. Such an equipotential pattern is shown here in Figure 4a. Figures 4b and 4c pertain to the conditions when IMF B_y is positive and negative, respectively, under southward IMF B_z. When IMF B_y was duskward (IMF B_{y+}), the banana-shaped dawn cell rotated in the premidnight sector as shown in Figure 4b bringing both Thumba and Jicamarca inside the same cell. The expected positions and movements of the electrodynamic divider ($\Phi = 0$) at certain times of observation along with its clock/anticlockwise rotations are also marked in Figures 4b and 4c. As the Indian sector went deeper inside the dawn cell with increasing IMF B_{y+} values, Thumba started experiencing enhanced eastward electric field perturbations. Jicamarca is believed to be well within the dawn cell during this period. This seems to be the case during $T_2 - T_3$. However, during $T_3 - T_4$, Jicamarca started coming out of the dawn cell that reduced the eastward electric field magnitude at this time.

In order to garner clue/support for the rotation of the high-latitude convection patterns during $T_2 - T_4$, a series of ionospheric convection maps generated based on the observations of Super Dual Auroral Radar Network (SuperDARN) of HF radars are investigated. Figures 5 and 6 capture a few important features of these observations made during 13:58 – 15:06 UT. Figure 5 shows that the dusk cell (in blue) is orange-like and the dawn cell (in red) is banana-like in Figures 5a and 5b. In this interval, IMF B_z became increasingly southward
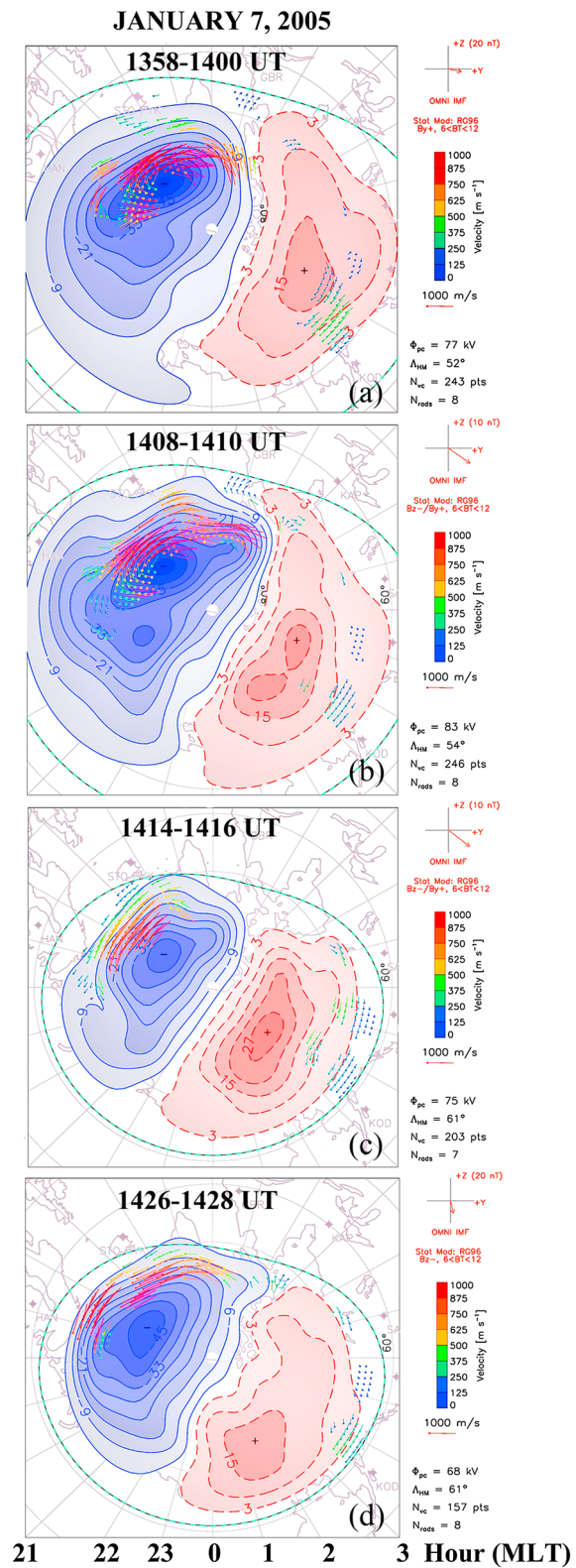
Figure 5. SuperDARN ionospheric convection maps along with DP2 contours during (a) 13:58–14:00 UT, (b) 14:08–14:10 UT, (c) 14:14–14:16 UT, and (d) 14:26–14:28 UT. Figures 5a and 5b show that the dusk cell (in blue) is orange-like and the dawn cell (in red) is banana-like. In this interval, IMF B_z becomes increasingly southward and IMF B_y is positive. In Figures 5c and 5d, although the sizes of the dawn and dusk cells become nearly same, the electrodynamical divider between these cells undergoes a clockwise rotation from the original noon-midnight line.
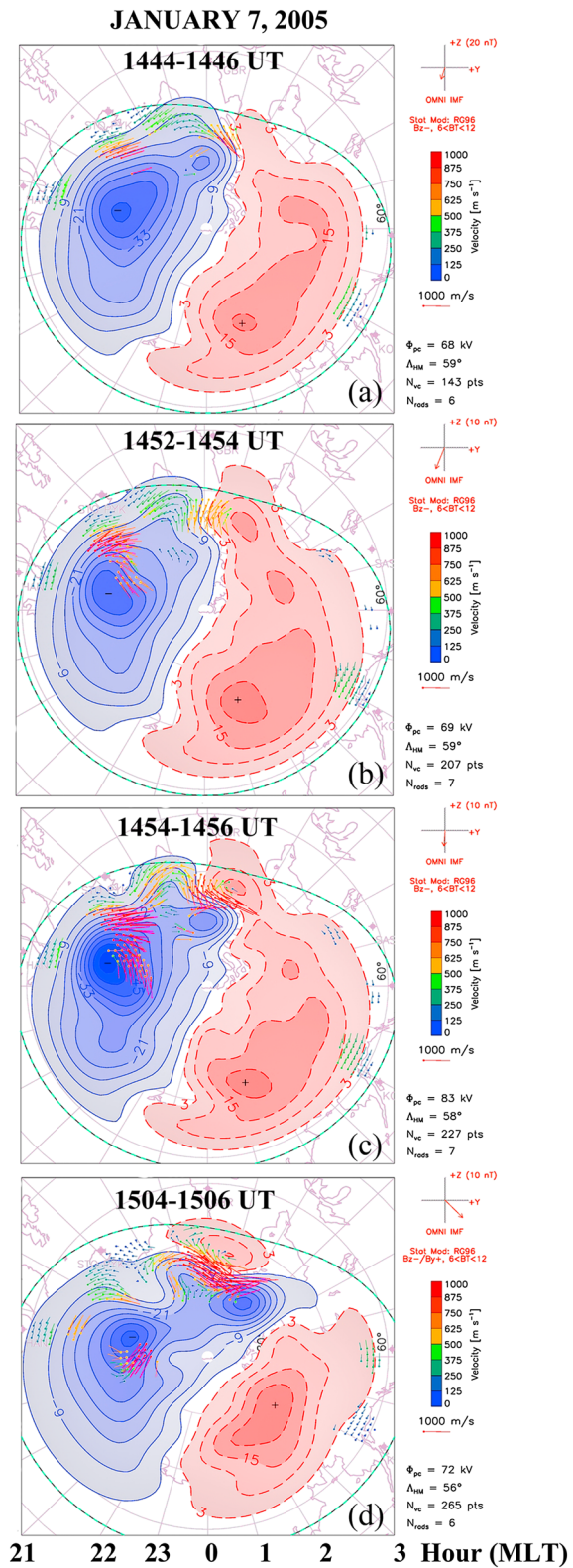
Figure 6. Same as Figure 5 but for intervals (a) 14:44–14:46 UT, (b) 14:52–14:54 UT, (c) 14:54–14:56 UT, and (d) 15:04–15:06 UT. Figures 6a and 6b reveal that the electrodynamical divider undergoes an anticlockwise rotation and IMF B_y is negative during this time. When IMF B_y suddenly takes a sharp positive turn, the electrodynamical divider again rotates clockwise and the dusk cell becomes orange-like. Figures 6c and 6d capture these features. It is at this time that Thumba experiences an enhanced eastward electric field. At this time IMF B_y is positive and IMF B_z is southward.

and IMF B_y was positive. In Figures 5c and 5d, although the sizes of the dawn and dusk cells became nearly the same, the electrodynamical divider between these cells underwent a clockwise rotation from the original noon-midnight line (see Figure 5a). This is consistent with positive IMF B_y effect [e.g., *Ruohoniemi and Greenwald*, 2005; *Tanaka*, 2007]. It is important to note that Thumba started experiencing the eastward electric field perturbation although the polarity did not fully become eastward at this time probably because the PP electric field was not sufficient to overcome quiet time dynamo electric field. The subplots in Figures 6a and 6b reveal that the electrodynamical divider now underwent an anticlockwise rotation and interestingly; IMF B_y became negative during this time. Strikingly, when IMF B_y suddenly took a sharp positive turn at ($T_3 - 00:10$), the electrodynamical divider again rotated clockwise and the dusk cell became orange-like. The subplots (6c and 6d) in Figure 6 capture these features. It was at this time that Thumba experienced an enhanced eastward electric field. As already stated, this is an expected outcome of positive IMF B_y under southward IMF B_z condition. Therefore, it is expected that changes in IMF B_y would also alter the distribution of equipotential contours in the dip equatorial ionosphere. This gets support from the magnetic measurements presented in Figure 3.

Kelley and Makela [2002] used Jicamarca data to report an anomalous eastward electric field polarity during postsunset hours and explained it as a modulating effect of positive IMF B_y. The present study not only supports that observation but further shows that identical polarity of the PP electric field can be experienced over Jicamarca and Indian sectors simultaneously under positive IMF B_y condition. It may also be noted that the effects of IMF B_y is generally not expected to be significant over equatorial ionosphere under northward IMF B_z conditions and hence not explored in the present investigation. The present study is the first of its kind as it shows the effects of changing IMF B_y (under southward IMF B_z condition) on the equatorial ionosphere by bringing in a number of global observations and drawing a larger picture. The present work automatically leads to the question as to what happens to curl-free condition of ionospheric electric field [*Fejer et al.*, 2008b; *Fejer*, 2011] under the circumstances when electric field perturbation of identical polarity is observed over the antipodal points like Jicamarca and Thumba. It can be noticed at this juncture that the plasma drifts depicted in Figures 1e and 1f during magnetically quiet time (in dashed blue) are of opposite polarities which is consistent with the general expectation of the vanishing of the closed line integral (curl-free condition) of ionospheric electric field. This is expected to be maintained even during magnetically disturbed condition. A similar polarity over Thumba and Jicamarca suggests that both the stations are on the same side of the electrodynamical boundary of the DP2 cells. Nevertheless, this does not violate the curl-free condition of the ionospheric electric field. In other words, the vertical plasma drifts will readjust among all longitudes along the dip equator so as to maintain the curl free condition: $\oint B V_z \mathrm{d}l = 0$, where B and V_z are the equatorial magnetic field strength and the vertical plasma drifts, respectively.

4. Summary

It is shown that the equatorial ionospheric electric field variations on 7 January 2005 consisted of a number of prompt penetration electric field effects with characteristic differences. In general, prompt penetration electric field perturbations of opposite polarities affect the equatorial ionosphere over Indian and Peruvian sectors. In contrast, the observed resultant (quiet time dynamo field $\pm$ prompt perturbation fields) electric fields over nearly antipodal points like Jicamarca and Thumba during 14:45–15:30 UT were both eastward. Investigating the reasons for such anomalous eastward electric field over Thumba, which was in sunset sector, it is observed that the high-latitude convection patterns show characteristic modifications in response to changes in the IMF B_y under southward IMF B_z conditions during this particular time interval. The examination of the X component of the magnetic field variations obtained from the chain of magnetometers in Indian and American longitude sectors shows that the effects of IMF B_y on these convection patterns were communicated to the low latitudes during 14:10–15:10 UT. It is suggested that distortion of the DP2 cells and the rotation of the electrodynamical boundary between the dawn and dusk cells because of IMF B_y changes under southward IMF B_z condition can lead to anomalous electric field behavior over equatorial antipodal points. It is observed that the effects of IMF B_y are not seen over low latitudes on either side of 14:10–15:10 UT even when IMF B_y is significant. Also, the present investigation shows such effects in the morning-postsunset sector only; it requires further investigations to understand under which circumstances and in which time sectors the IMF B_y effects are communicated to low latitudes.

References

Bhaskar, A., and G. Vichare (2013), Characteristics of penetration electric fields to the equatorial ionosphere during southward and northward IMF turnings, *J. Geophys. Res. Space Physics*, 118, 4696–4709, doi:10.1002/jgra.50436.

Bittencourt, J. A., and M. A. Abdu (1981), A theoretical comparison between apparent and real vertical ionization drift velocities in the equatorial F region, *J. Geophys. Res.*, 86(A4), 2451–2454, doi:10.1029/JA086iA04p02451.

Chakrabarty, D., R. Sekar, R. Narayanan, C. V. Devasia, and B. M. Pathan (2005), Evidence for the interplanetary electric field effect on the OI 630.0 nm airglow over low latitude, *J. Geophys. Res*, 110, A11301, doi:10.1029/2005JA011221.

Chakrabarty, D., R. Sekar, R. Narayanan, A. K. Patra, and C. V. Devasia (2006), Effects of interplanetary electric field on the development of an equatorial spread F event, *J. Geophys. Res*, 111, A12316, doi:10.1029/2006JA011884.

Chakrabarty, D., R. Sekar, J. H. Sastri, B. M. Pathan, G. D. Reeves, K. Yumoto, and T. Kikuchi (2010), Evidence for OI 630.0 nm dayglow variations over low latitudes during onset of a substorm, *J. Geophys. Res*, 115, A10316, doi:10.1029/2010JA015643.

Chakrabarty, D., D. Rout, R. Sekar, R. Narayanan, G. D. Reeves, T. K. Pant, B. Veenadhari, and K. Shiokawa (2015), Three different types of electric field disturbances affecting equatorial ionosphere during a long-duration prompt penetration event, *J. Geophys. Res. Space Physics*, 120, 4993–5008, doi:10.1002/2014JA020759.

Cumnock, J. A., R. A. Heelis, and M. R. Hairston (1992), Response of the ionospheric convection pattern to a rotation of the interplanetary magnetic field on January 14, 1988, *J. Geophys. Res*, 97(A12), 19,449–19,460, doi:10.1029/92JA01731.

Cumnock, J. A., J. R. Sharber, R. A. Heelis, M. R. Hairston, and J. D. Craven (1997), Evolution of the global aurora during positive IMF B_z and varying IMF B_y conditions, *J. Geophys. Res.*, 102(A8), 17,489–17,497, doi:10.1029/97JA01182.

Fejer, B. G. (2011), Low latitude ionospheric electrodynamics, *Space Sci. Rev*, 158(1), 145–166, doi:10.1007/s11214-010-9690-7.

Fejer, B. G., J. W. Jensen, and S.-Y. Su (2008a), Seasonal and longitudinal dependence of equatorial disturbance vertical plasma drifts, *Geophys. Res. Lett.*, 35, L20106, doi:10.1029/2008GL035584.

Fejer, B. G., J. W. Jensen, and S.-Y. Su (2008b), Quiet time equatorial F region vertical plasma drift model derived from ROCSAT-1 observations, *J. Geophys. Res.*, 113, A05304, doi:10.1029/2007JA012801.

Friis-Christensen, E., Y. Kamide, A. D. Richmond, and S. Matsushita (1985), Interplanetary magnetic field control of high-latitude electric fields and currents determined from Greenland Magnetometer Data, *J. Geophys. Res.*, 90(A2), 1325–1338, doi:10.1029/JA090iA02p01325.

Gonzales, C., M. Kelley, B. Fejer, J. Vickrey, and R. Woodman (1979), Equatorial electric fields during magnetically disturbed conditions: 2. Implications of simultaneous auroral and equatorial measurements, *J. Geophys. Res.*, 84(A10), 5803–5812, doi:10.1029/JA084iA10p05803.

Heelis, R. A. (1984), The effects of interplanetary magnetic field orientation on dayside high-latitude ionospheric convection, *J. Geophys. Res.*, 89(A5), 2873–2880, doi:10.1029/JA089iA05p02873.

Huang, C.-S. (2008), Continuous penetration of the interplanetary electric field to the equatorial ionosphere over eight hours during intense geomagnetic storms, *J. Geophys. Res.*, 113, A11305, doi:10.1029/2008JA013588.

Hui, D., and B. G. Fejer (2015), Daytime plasma drifts in the equatorial lower ionosphere, *J. Geophys. Res. Space Physics*, 120, 9738–9747, doi:10.1002/2015JA021838.

Kelley, M. C., and J. J. Makela (2002), By dependent prompt penetrating electric fields at the magnetic equator, *Geophys. Res. Lett.*, 29(7), 571–573, doi:10.1029/2001GL014468.

Kelley, M. C., M. J. Nicolls, D. Anderson, A. Anghel, J. L. Chau, R. Sekar, K. S. V. Subbarao, and A. Bhattacharyya (2007), Multi-longitude case studies comparing the interplanetary and equatorial ionospheric electric fields using an empirical model, *J. Atmos. Terr. Phys.*, 69(10–11), 1174–1181, doi:10.1016/j.jastp.2006.08.014.

Kikuchi, T., K. K. Hashimoto, and K. Nozaki (2008), Penetration of magnetospheric electric fields to the equator during a geomagnetic storm, *J. Geophys. Res.*, 113, A06214, doi:10.1029/2007JA012628.

Kikuchi, T., Y. Ebihara, K. K. Hashimoto, R. Kataoka, T. Hori, S. Watari, and N. Nishitani (2010), Penetration of the convection and overshielding electric fields to the equatorial ionosphere during a quasiperiodic DP 2 geomagnetic fluctuation event, *J. Geophys. Res.*, 115, A05209, doi:10.1029/2008JA013948.

Kudeki, E., and C. D. Fawcett (1993), High resolution observations of 150 km echoes at Jicamarca, *Geophys. Res. Lett.*, 20(18), 1987–1990, doi:10.1029/93GL01256.

Kullen, A., R. C. Fear, S. E. Milan, J. A. Carter, and T. Karlsson (2015), The statistical difference between bending arcs and regular polar arcs, *J. Geophys. Res. Space Physics*, 120, 10,443–10,465, doi:10.1002/2015JA021298.

Lee, D.-Y., L. R. Lyons, and G. D. Reeves (2005), Comparison of geosynchronous energetic particle flux responses to solar wind dynamic pressure enhancements and substorms, *J. Geophys. Res.*, 110, A09213, doi:10.1029/2005JA011091.

Madhav Haridas, M. K., G. Manju, and T. K. Pant (2015), On the solar activity variations of nocturnal F region vertical drifts covering two solar cycles in the Indian longitude sector, *J. Geophys. Res. Space Physics*, 120, 1445–1451, doi:10.1002/2014JA020561.

Maruyama, N., A. D. Richmond, T. J. Fuller-Rowell, M. V. Codrescu, S. Sazykin, F. R. Toffoletto, R. W. Spiro, and G. H. Millward (2005), Interaction between direct penetration and disturbance dynamo electric fields in the storm-time equatorial ionosphere, *Geophys. Res. Lett.*, 32, L17105, doi:10.1029/2005GL023763.

Nopper, R. W., and R. L. Carovillano (1978), Polar-equatorial coupling during magnetically active periods, *Geophys. Res. Lett.*, 5(8), 699–702, doi:10.1029/GL005i008p00699.

Pandey, K., R. Sekar, B. Anandarao, S. Gupta, and D. Chakrabarty (2016), Estimation of nighttime dip-equatorial E-region current density using measurements and models, *J. Atmos. Terr. Phys*, 146, 160–170, doi:10.1016/j.jastp.2016.06.002.

Rastogi, R. G., H. Chandra, and M. E. James (1996), Nocturnal variations of geomagnetic horizontal field at equatorial stations, *Geophys. Res. Lett.*, 23(19), 2601–2604, doi:10.1029/96GL02390.

Reeves, G., et al. (2003), IMAGE, POLAR, and geosynchronous observations of substorm and ring current ion injection, in *Disturbances in Geospace: The Storm-Substorm Relationship, Geophys. Monogr. Ser.*, vol. 142, pp. 91–101, AGU, Washington, D. C.

Ruohoniemi, J. M., and R. A. Greenwald (2005), Dependencies of high-latitude plasma convection: Consideration of interplanetary magnetic field, seasonal, and universal time factors in statistical patterns, *J. Geophys. Res.*, 110, A09204, doi:10.1029/2004JA010815.

Sekar, R., and D. Chakrabarty (2008), Role of overshielding electric field on the development of pre-midnight plume event: Simulation results, *J. Atmos. Terr. Phys*, 70(17), 2212–2221, doi:10.1016/j.jastp.2008.04.015.

Senior, C., and M. Blanc (1984), On the control of magnetospheric convection by the spatial distribution of ionospheric conductivities, *J. Geophys. Res.*, 89(A1), 261–284, doi:10.1029/JA089iA01p00261.

Simi, K. G., S. V. Thampi, D. Chakrabarty, B. M. Pathan, S. R. Prabhakaran Nayar, and T. Kumar Pant (2012), Extreme changes in the equatorial electrojet under the influence of interplanetary electric field and the associated modification in the low-latitude F region plasma distribution, *J. Geophys. Res.*, 117, A03331, doi:10.1029/2011JA017328.

Tanaka, T. (2007), Magnetosphere-ionosphere convection as a compound system, *Space Sci. Rev.*, *133*(1), 1–72, doi:10.1007/s11214-007-9168-4.

Tsunomura, S. (1999), Numerical analysis of global ionospheric current system including the effect of equatorial enhancement, *Ann. Geophys.*, *17*(5), 692–706, doi:10.1007/s00585-999-0692-2.

Tsunomura, S., and T. Araki (1984), Numerical analysis of equatorial enhancement of geomagnetic sudden commencement, *Planet. Space Sci.*, *32*(5), 599–604, doi:10.1016/0032-0633(84)90109-0.

Tsurutani, B. T., et al. (2008), Prompt penetration electric fields (PPEFs) and their ionospheric effects during the great magnetic storm of 30–31 October 2003, *J. Geophys. Res.*, *113*(A5), A05311, doi:10.1029/2007JA012879.

Vasyliunas, V. M. (1970), *Mathematical Models of Magnetospheric Convection and its Coupling to the Ionosphere*, pp. 60–71, Springer, Dordrecht, Netherlands, doi:10.1007/978-94-010-3284-16.

Wolf, R., and R. Jaggi (1973), Can the magnetospheric electric field penetrate to the low-latitude ionosphere, *Commun. Astrophys. Space Phys.*, *5*, 99.